First-principles study of intrinsic defects in yttrium oxysulfide

Masayoshi Mikami*
Yokohama Research Center, Mitsubishi Chemical Corporation, 1000 Kamoshida-cho, Aoba-ku, Yokohama 227-8502, Japan

Atsushi Oshiyama
Institute of Physics, University of Tsukuba, 1-1-1 Tennodai, Tsukuba 305-8571, Japan
(Received 6 October 1998)

Atomic and electronic structures of intrinsic point defects in yttrium oxysulfides (Y_2O_2S) are studied by first-principles total-energy calculations based on density-functional theory combined with normconserving pseudopotentials. Energetics of all the intrinsic point defects are determined for a variety of charge states. From the energetics, the concentrations of the anion vacancies and the interstitial anions are found to be larger than those of the yttrium vacancy and the interstitial yttrium atom under practical conditions. It is also found that the oxygen vacancy, the sulfur vacancy, and the interstitial sulfur atom induce relatively deep levels in the energy gap, whereas the interstitial oxygen atom induces relatively shallow acceptor levels. These findings are consistent with observed broad-band blue luminescence in undoped yttrium oxysulfide, existence of shallow acceptor levels in oxysulfides, and are presumably related to persistent phosphorescence and energy storage phenomena in Eu-doped oxysulfides. Furthermore, negative-*U* characters are found in the oxygen vacancy and the interstitial sulfur. These behaviors of the defects can be explained from the viewpoint of the covalent bonds newly appearing around the defects in the ionic host material. [S0163-1829(99)03627-9]

I. INTRODUCTION

Defects in semiconductors generally affect optical and electronic properties of the host materials. In wide-gap semiconductors that are mainly applied to blue or ultraviolet light-emitting diodes, a variety of defect-related phenomena such as luminescence from deep levels, self-compensation, uniporality, and so on are certainly observed; ''yellow luminescence'' in GaN, for example, is supposed to be a transition from a shallow donor level to a deep acceptor level induced by gallium vacancy.[1,2] Control of the defects is thus of principal importance in technology. In this respect, defect formation energy (DFE) defined as energy cost to make a defect, has an important meaning. The DFE's in wide-gap semiconductors are sensitive to their charge states; DFE's may vary by the order of the wide-band gap upon electron transfer to or from the Fermi level. Therefore, understanding and, if possible, control of their intrinsic defects for a variety of charge states are essential to exploit potentialities of wide-gap materials. The aim of the present paper is to study the electronic structure of intrinsic point defects for a variety of charge states in yttrium oxysulfide (Y_2O_2S), which is also a wide-gap semiconductor.

Rare-earth oxysulfides (M_2O_2S with $M=Y$, and the lanthanides, space group $P\bar{3}m1$, Fig. 1) are known as wide-gap (4.6–4.8 eV) semiconductors.[3] They have been utilized as host materials for efficient phosphorescent use about a quarter of a century.[4] Especially, europium-activated Y_2O_2S emits bright red light under cathode-ray excitation and have been widely used for televisions.[5,6] From the scientific viewpoints, the rare-earth oxysulfides are unique in their characters. The rare-earth atom usually contains *d* orbitals as its valence states so that unusual many fold hybridization is expected in oxysulfides. Electron transfer from the rare-earth atom to sulfur and oxygen atoms is also expected. Delicate difference in ionicity between the sulfur and the oxygen atoms is also of interest.

In our previous work,[7] we have investigated the electronic structure of crystalline Y_2O_2S by first-principles total-energy electronic-structure calculations. We have found that Y_2O_2S is an indirect-gap semiconductor and the band structure is substantially anisotropic, which is in accord with the observed anisotropic character of its refractive index. We have also clarified that there is higher electron density around oxygen atoms than around sulfur atoms, and that substantial covalency in Y-O bonds and less covalency in Y-S bonds coexist. The degree of the covalency is also understandable from the comparison between the bond length and the sum of the corresponding Pauling's ionic radii.[8] From the chemical

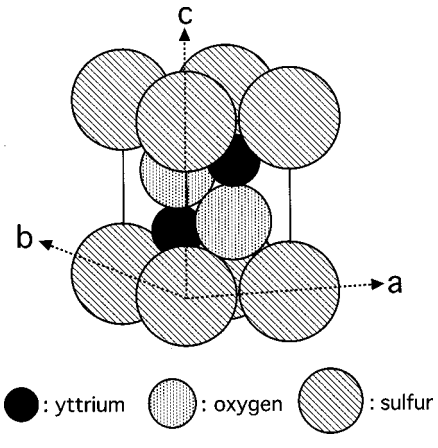

FIG. 1. Crystal structure of M_2O_2S ($M=Y$ and lanthanides). (trigonal, $P\bar{3}m1$) Sizes of the atoms are shown according to Pauling's ionic radii (Ref. 8); 0.96, 1.40, and 1.84 Å for yttrium, oxygen, and sulfur atoms, respectively. Calculated lattice constants *a* and *c* are 3.750 and 6.525 Å, respectively.

difference between the O and the S atoms in Y_2O_2S, we expect different properties between the sulfur and the oxygen vacancy in this material. Or more generally, the intrinsic point defects in Y_2O_2S are expected to have unique characters due to the competition between covalency and ionicity. It is, therefore, interesting to investigate the intrinsic defects in such an exotic system with first-principles methods.

Some defects in the oxysulfides, in fact, have been supposed to play important roles in several interesting phenomena for a long time. To begin with, there are several indications that intrinsic shallow acceptor levels exist in oxysulfides. Dobrov and Buchanan observed that rare-earth element (Eu, Tb, Nd) doped lanthanum oxysulfides exhibited strong photoconductivity under ultraviolet (UV) light.[9] The gradual increase in the photoconductive response in the 250–300 nm region in all the samples suggests that the photoconductivity is associated with the host property of the lanthanum oxysulfides. This photoconduction strongly increases with increasing temperature. This suggests that carrier lifetime is limited by traps. The majority of photocarriers have been identified as holes by measuring the sign of the Hall photovoltage. The doped rare-earth ions are expected to have the same charge state as Y ion (+3) in the oxysulfides, i.e., isovalent impurities, so that the hole conduction have been speculated to come from shallow acceptor levels induced by intrinsic defects of the oxysulfides.

As for phenomena presumably related to the shallow acceptor levels, we mention two examples; persistent phosphorescence and energy storage phenomena in Eu-doped oxysulfides. It has been known that Eu-doped oxysulfides excited by x-rays or cathode rays show phosphorescence that lasts many minutes even at room temperature, while Eu^{3+} transition ($^5D_J \rightarrow {}^7F_{J'}$) has a radiative lifetime no longer than a few milliseconds.[10] Further, an interesting energy-storage phenomenon in oxysulfides has been observed by Forest *et al.*[11] and Struck *et al.*;[12] energies used to excite the materials can be stored for months in appropriate conditions (e.g., below 200 K in La_2O_2S), and then be released as Eu radiative transitions either by infrared (IR) or thermal stimulation. Struck and Fonger proposed that both the persistent phosphorescence and the energy storage are related to shallow acceptor levels: i.e., the excited Eu^{3+} level, charge-transfer state, becomes Eu^{2+} plus a free hole; the hole is trapped at the shallow level; upon IR or thermal excitation, the hole is now released from the level; the resultant free hole subsequently recombine with Eu^{2+} and then the radiative transition in Eu^{3+} ion occurs.[10]

Moreover, defect-related luminescence is also observed. Especially, Yamamoto *et al.* found broad blue luminescence bands with peaks at around 355 and 440 nm (3.5 and 2.8 eV, respectively) at 80 K in undoped Y_2O_2S.[13] Considering its band-gap value (around 4.6 eV), we speculate that deep levels play important roles in this phenomena. The similarity with the yellow luminescence in *n*-type GaN may be interesting.

In spite of all these experimental efforts, no microscopic identification has been achieved for various defect levels in Y_2O_2S. No theoretical studies have been ever tried to propose plausible microscopic models for the above phenomena.

In this paper, we report the first *ab initio* calculations of atomic and electronic structures and the energetics of intrinsic defects in yttrium oxysulfides. These types of calculations have only recently been applied to the study of wide gap materials.[2,14–18] We have calculated DFE's of intrinsic defects for a variety of charge states: the oxygen vacancy (V_O), the sulfur vacancy (V_S), the yttrium vacancy (V_Y), the interstitial oxygen atom (O_{int}), the interstitial sulfur atom (S_{int}), and the interstitial yttrium atom (Y_{int}). From the DFE's, the concentration of the anion-related defects are found to be much lager and thus to play more important roles in physical phenomena than the yttrium-related defects. We have also explored induced single-electron energy levels in the band gap and have found that the anion vacancies and the interstitial sulfur induce relatively deep levels in the band gap, whereas the interstitial oxygen does a shallow acceptor level. We, thus, expect that broad-band blue luminescence observed in undoped yttrium oxysulfide stems from these deep levels and that the O_{int}-induced shallow acceptor level is responsible for the hole photoconduction, the persistent phosphorescence and the energy-storage phenomenon. Further, we have also found that the oxygen vacancy, the interstitial sulfur, and the interstitial yttrium have negative-*U* characters: covalent bonds appearing around the defects play an important role in this ionic host material.

The organization of the present paper is as follows: In Sec. II, we present a brief explanation of the first-principle band-structure calculations using normconserving pseudopotentials and the definition of DFE, in Secs. III and IV the calculated results and discussion are shown, respectively. Section V concludes the paper.

II. CALCULATION METHOD

We perform total-energy electronic-structure calculations based on density-functional theory with local-density approximation (LDA) combined with normconserving pseudopotentials.[19–22] Troullier-Martins-type normconserving pseudopotentials[23] are generated to simulate nuclei and core electrons, where we use fully separable Kleinman-Bylander-type pseudopotentials.[24] Yttrium pseudopotential is generated from an atomic configuration $5s^2 4d^1 5p^0$ with core radii of 3.11, 3.47, and 2.07 a.u. for the *s*, *p*, and *d* components, respectively. The sulfur pseudopotential is generated from the atomic configuration $3s^2 3p^4 3d^0$ with core radii of 1.54, 1.78, and 1.78 a.u. for the *s*, *p*, and *d* components, respectively. For the oxygen pseudopotential, the configuration of $2s^2 2p^4$ with core radii of 1.41 and 1.41 a.u. for the *s* and *p* components, respectively, is used. Interaction among valence electrons are treated within the LDA: we use the exchange-correlation functional of Ceperley and Alder[25] as parameterized by Perdew and Zunger.[26] We have found that the calculated equilibrium volume and internal coordinates of atoms agree well with experimental results even without partial-core correction;[7] the calculated lattice constants *a* and *c* are 3.750 and 6.525 Å , respectively; atom positions in Y_2O_2S using the lattice vector unit are $\pm(0.333,0.667,0.282)$ for two yttrium atoms, $\pm(0.333,0.667,0.631)$ for two oxygen atoms, and (0,0,0) for a sulfur atom. These calculated parameters agree well with the experimental ones within 1% errors. Further detailed accounts can be found in our previous work.[7]

For a variety of charge states of defects, we calculate total ground-state energies and atomic forces, search (meta-)stable atomic geometries, and then obtain electronic structures in the resulting (meta-)stable atomic geometries. A point defect in an otherwise perfect crystal is simulated by a supercell that contains 40 lattice sites ($2a\times 2a\times 2c$);[27] the lattice constants, a and c, are set to be the above theoretical values. In the case of the vacancy, we make its initial geometry by just removing an atom from the supercell. In the case of the interstitial atom, we put an interstitial atom at the midpoint between two sulfur atoms along c axis for initial geometry; from the Pauling's ionic radii[8] of the atoms (see Fig. 1), this site has the widest space in which the interstitial atoms could occupy. We then optimize each (charged-)defect geometry by minimizing its total energy without any assumptions of geometrical symmetry. Wave functions and thus charge densities are expanded in terms of plane-wave basis set. The cutoff energy of the plane-wave basis set is 59 Ry, which is adequate for obtaining converged results in these calculations.[28] Γ-point sampling is used for the Brillouin zone integration; the geometries optimized with the Γ-point sampling remain unchanged when we use the three special k-point sampling.[29] The related error of the total-energy difference is also estimated to be less than 0.5 eV. This value is sufficiently smaller than the DFE difference among the intrinsic defects that we will discuss later. The conjugate gradient minimization technique[21] is employed to minimize the total energy with respect to both electronic and ionic degrees of freedom. In the resulting (meta-)stable geometries, the force acting on each atom is less than, typically, 0.008 Ry/Å. The formation energy $E_f(Q)$ of a point defect related to the atom species i (= Y, O, S) in Y_2O_2S with the charge state $Q(=0,\pm 1,\pm 2,\ldots)$ is defined as

$$E_f(Q)=\Delta E_{\rm tot}(Q)\pm\mu_{\rm i}+Q(\mu_e+E_v^Q), \qquad (2.1)$$

where in the plus-minus sign the $+$ corresponds to a vacancy and the $-$ to an interstitial atom, and μ_e and μ_i are the electron chemical potential and the atom chemical potential, respectively. Here, Q conventionally corresponds to the number of electrons transferred from the defect to a reservoir of electrons, and $\Delta E_{\rm tot}(Q)$ is the total energy difference between the supercell containing the defect with the charge state Q and the perfect crystal supercell, i.e., $E_{\rm tot}(Q)-E_{\rm crys}$. The zero of μ_e is defined as the top of valence-band energy E_v^Q of the defect supercell with the charge state Q. In this definition, the DFE has the meaning of energy cost to make an point defect in the crystal.

As expressed above, the formation energy depends on the charge state, the Fermi level (μ_e), and on the atomic chemical potential μ_i (i=Y,O,S). The μ_e is determined by doping conditions and is also related to concentrations of other defects and to the number of externally injected carriers. In this paper, we simply regard it as an external parameter. The μ_i is generally determined by an equilibrium condition and kinetic hindrances in growth processes. The equilibrium condition leads to

$$\mu_{Y_2O_2S}=2\mu_Y+2\mu_O+\mu_S, \qquad (2.2)$$

where $\mu_{Y_2O_2S}$ is the chemical potential of Y_2O_2S. In this paper, we adopt the μ_O (μ_S) to be one half of the total energy of the spin-unpolarized O_2 (S_2) molecule.[30] This setting of the chemical potentials corresponds to a situation in which Y_2O_2S is exposed to the atmosphere of O_2 and S_2 during the growth. We think that this setting is quite practical.[31]

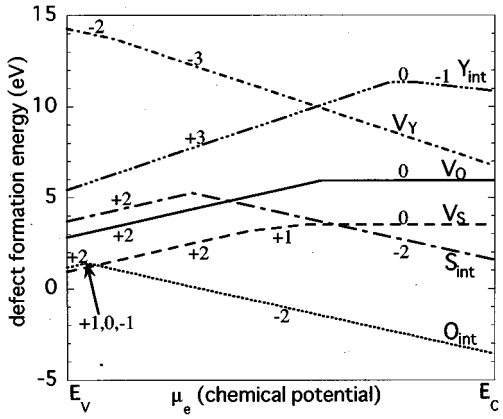

FIG. 2. Defect formation energies (DFE's) for O- (V_O), S- (V_S), and Y- (V_Y) vacancies and for interstitial O ($O_{\rm int}$), S ($S_{\rm int}$), and Y ($Y_{\rm int}$). The chemical potentials are set by $\mu_{Y_2O_2S}=2\mu_Y+2\mu_O+\mu_S, 2\mu_O=\mu_{O_2}$, and $2\mu_S=\mu_{S_2}$. E_V and E_C stand for the top of valence bands and the bottom of conduction bands in our calculation, respectively. The calculated band gap is 2.61 eV in our previous work. The signed numbers stand for the charge states of the defects.

We here add a comment on the technique in dealing with charge states. In the calculation for the charge state Q, an uniform background charge with opposite sign is distributed to keep neutrality of the whole system (this prescription prevents the divergence in the calculated total energies). In this calculation, the total energy $E_{\rm tot}(Q)$ is underestimated because of the fictitious attractive interaction between the background charge and the excess charge Q, while the total energy $E_{\rm tot}(0)$ in a noncharged system is well defined. In order to correct this underestimation, we estimate the total energy of the charged states according to the ''Slater's transition-state theory.''[32]

III. RESULTS

A. Energetics of defects from DFE diagram

In this section we present calculated DFE's of intrinsic point defects in Y_2O_2S for a variety of charge states. Figure 2 shows DFE's as a function of the electron chemical potential in the calculated energy gap of Y_2O_2S (2.61 eV). As for vacancies, it is found that the sulfur vacancy V_S is lower than the oxygen vacancy V_O in formation energy at any position of the electron chemical potential in the energy gap, and that the DFE of yttrium vacancy V_Y is the highest. The formation energies of the V_S and the V_O for their neutral charge states are 3.51 and 5.93 eV, respectively.[33] This difference is understandable from the difference in properties between the Y-O bond and the Y-S bond in crystalline Y_2O_2S: It has been clarified[7] that the Y-O bond is more covalent than the Y-S bond. This strength difference between the Y-O bond and the Y-S bond presumably leads to the difference be-

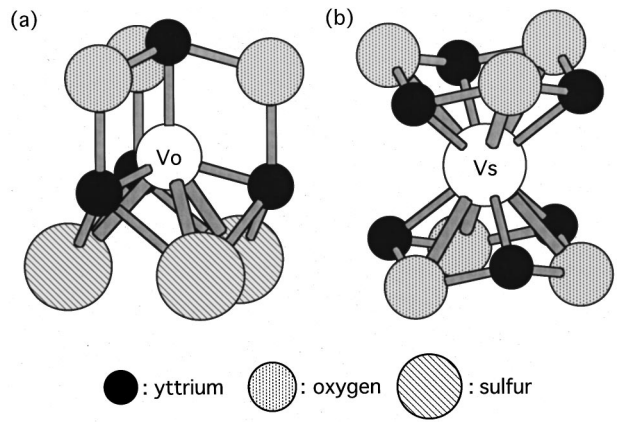

FIG. 3. Schematic views of atomic arrangements around (a) the oxygen vacancy and (b) the sulfur vacancy.

tween their DFE's. Compared with these anion vacancies, the DFE of V_Y is much larger. This is because one Y atom in Y_2O_2S forms four bonds with neighboring O atoms and three bonds with the neighboring S atoms. We, thus, reasonably expect that the concentration of V_Y is much smaller than those of the O and S vacancies.[31] Moreover, we find that the V_O is the negative-U system. In Fig. 2, it is clear that the V_O with the singly positive charge state ($V_O^{(+1)}$) is metastable at any position of μ_e in the energy gap. Either $V_O^{(+2)}$ or $V_O^{(0)}$ is the most stable form of the V_O. (Here, the superscripts depict the charge state.) This is again due to the strong covalency and the resulting electron-lattice (E-L) interaction around the V_O. We will return to this point later.

As for interstitial atoms, it is found that the interstitial atoms has a variety of charge states: $Q=-2$, -1, 0, $+1$, or $+2$ for the oxygen interstitial O_{int}, $Q=-2$ or $+2$ for the sulfur interstitial S_{int}, and $Q=+3$, 0, or -1 for the yttrium interstitial Y_{int} (the $Q=-1$, 0, and $+1$ states for O_{int} are stable in an extremely small region of μ_e in Fig. 2). The formation energy of the O_{int} is the lowest: the calculated DFE's for the neutral charge state are 1.36 eV for O_{int}, 5.47 eV for S_{int} and 11.34 eV for Y_{int}, respectively. The much larger DFE of Y_{int} than the others seems to come from the fact that the bond lengths between Y_{int} and the surrounding yttrium atoms (from 2.720 Å for $Q=-1$ to 2.878 Å for $Q=+3$) are 24% shorter than the ones in hcp yttrium metal (3.555,3.645 Å). The difference of DFE's between O_{int} and S_{int} will be explained later from the bonding around the interstitial atoms. Again, the S_{int} and the Y_{int} are the negative-U system in the sense that intermediate charge states are metastable at any position of the Fermi level μ_e. This finding also indicates the strong hybridization and the resulting E-L interaction around the interstitial atoms.

From the calculated DFE's, the O_{int} and possibly the V_S are the most abundant intrinsic point defects in Y_2O_2S. Even if we consider the ambiguity of the chemical potentials of atomic species, concentrations of the V_Y and the Y_{int} are likely to be much smaller than that of other intrinsic defects.[31] We, thus, safely exclude the possibility that V_Y and Y_{int} play roles in explaining the defect-related phenomena, which we have mentioned in the Introduction.

TABLE I. The distances between the sulfur vacancy (V_S) site and the neighboring atoms in the total-energy minimized sulfur vacancy. Superscripts stand for charge states of the V_S. The distances in the initial (unrelaxed) configuration are also shown in the column "$V_S^{(init)}$." Units in Å.

Parameter	$V_S^{(0)}$	$V_S^{(+1)}$	$V_S^{(+2)}$	$V_S^{(init)}$
V_S-Y	2.836	2.889	2.928	2.834
V_S-O	3.213	3.172	3.089	3.231

B. Atomic and electronic structures of anion vacancies

We discuss the atomic and electronic structures of the vacancies in this subsection. Here, we focus mainly on the anion vacancies for the reason stated in the previous subsection.

We first examine the atomic structures around the anion vacancies. Schematic views around the anion vacancies are shown in Fig. 3. The geometry information is also given in Tables I and II. In the total-energy minimized neutral vacancies, the displacements of the neighboring atoms from the initial (unrelaxed) geometry in $V_O^{(0)}$ are larger than in $V_S^{(0)}$. Subsequently, the energy gain due to the relaxation of the surrounding atoms of $V_O^{(0)}$ is 0.37 eV, which is much larger than the corresponding value 0.07 eV in $V_S^{(0)}$. These are explained from the viewpoint of the atomic structures of the two vacancies; in the neutral state, the distances between the yttrium atoms adjacent to $V_O^{(0)}$ are 3.758 and 3.893 Å, much shorter than the counterparts in S vacancy (5.672 Å); the Y-Y distances in $V_O^{(0)}$ are longer than the distances between the nearest neighbor yttrium atoms in hcp yttrium metal (3.555,3.645 Å) only by 3%; this means that the strong hybridization between the yttrium atoms takes place in the V_O; from this respect, the reconstruction of the V_O, i.e., the yttrium-yttrium rebonding around the V_O, is stronger than that of the V_S. Further, we have found that the variation of the displacements of the neighboring atoms as a function of the charge state is larger in the V_O than in the V_S: When the charge state of V_S changed from $Q=0$ to $Q=+2$, the displacement of yttrium atom adjacent to the V_S is 0.092 Å; on the other hand, the corresponding displacement in the V_O is larger (0.178 Å). This larger displacement in the V_O implies the strong E-L coupling.

Figure 4 shows the calculated single electron levels in the energy gap. Occupancy levels that are measured in experiments are the total energy differences between different charge states. It is also known that to identify a difference in

TABLE II. The distances between the oxygen vacancy (V_O) site and the neighboring atoms in the total-energy minimized oxygen vacancy. Superscripts stand for charge states of the V_O. The distances in the initial (unrelaxed) configuration are shown in the column "$V_O^{(init)}$." Distances between yttrium atoms that surround V_O are also shown. Units in Å.

Parameter	$V_O^{(0)}$	$V_O^{(+1)}$	$V_O^{(+2)}$	$V_O^{(init)}$
V_O-Y	2.426,2.323	2.518,2.335	2.604,2.363	2.235,2.277
V_O-S	3.188	3.152	3.106	3.231
Y-Y	3.758,3.893	3.855,3.904	3.964,3.938	3.591,3.744

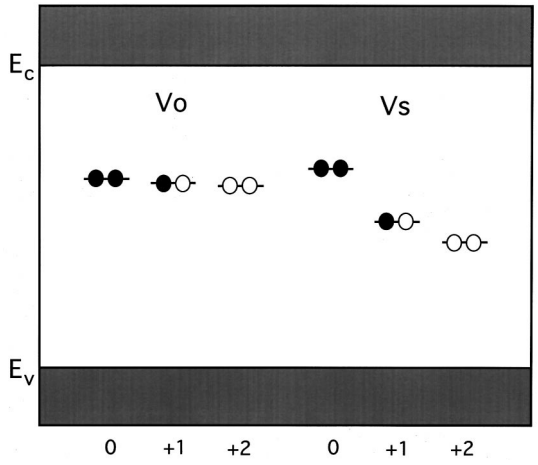

FIG. 4. Single-electron levels in the energy gap induced by the oxygen and sulfur vacancies. The signed numbers stand for charge states of the defects. Filled circles indicate electrons, and open circles indicate holes.

single electron levels obtained by the LDA as an excitation energy of the system causes a substantial error: e.g., the present LDA calculation gives 2.61 eV for the energy gap of Y_2O_2S, which is considerably smaller than the experimental gap ($\sim$4.6 eV). The positions of the levels induced by the defects in this subsection are thus of qualitative meaning. We can identify the character of each level by analyzing its wave function, and the analysis is useful to obtain chemical picture of the deep levels, however.

We first notice that the V_S and V_O each induce a deep single level in the energy gap. In their neutral charge states, two electrons occupy the level. Their charge state can be changed up to $Q=+2$ as we stated above. The $Q=+2$ charge state of V_O (V_S) corresponds to a removal of a doubly negatively charged oxygen (sulfur) anion from the perfect crystal. On the other hand, we find that the V_Y induces relatively (doubly degenerate) shallow acceptor levels in the gap. The degenerate levels are fully occupied in the $Q=-3$ charge state. This $Q=-3$ charge state of the V_Y corresponds to a removal of a triply positively charged yttrium cation from the crystal. These are in accord with a notion that Y_2O_2S is formally composed of Y^{+3} cations, O^{-2} anions, and S^{-2} anions.

Wave functions of the deep levels induced by the V_O and the V_S manifest their characteristics clearly. Figure 5 shows the wave functions of the deep levels induced by the anion vacancies. Both in the V_O and in the V_S, we find substantial amplitudes of wave functions between yttrium atoms neighboring to the vacancy. In the host of Y_2O_2S, approximately two electrons are transferred to an O (S) atom from surrounding four (six) yttrium atoms. Thus, removing one O (S) atom leaves two electrons behind and the electrons occupy the deep level. The deep level induced by the V_S or V_O consists of the $4d$ characters of the yttrium atoms surrounding the vacancies. That is why we observe the bonding between yttrium $4d$-like wave functions in Fig. 5. Moreover we find that the appearance of bonding is rather different between the V_S and the V_O: While the bonding between yttrium atoms adjacent to the V_S looks weak, the strong hybridization of yttrium atoms adjacent to the V_O is prominent.

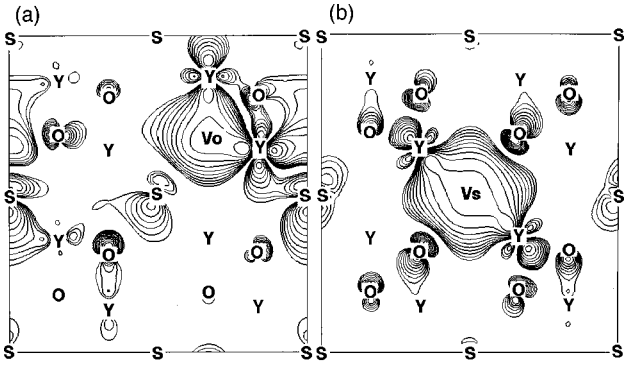

FIG. 5. Contour maps of wave functions of the defect levels for the oxygen and sulfur vacancies at Γ point; (a) oxygen vacancy and (b) sulfur vacancy. The subsequent contours represent the values different to each other by a factor of 1.5.

This comes from that the distance between the neighboring yttrium atoms around the V_O is much shorter than in the case of the V_S, as we stated before. This strong hybridization between yttrium $4d$-like wave functions in the V_O can explain the larger energy gain due to relaxation of surrounding atoms, the strong E-L coupling, and the resulting negative-U character.

We have also found the small energy shift of the deep level of the V_O when charge state of the V_O changes from $Q=0$ to $Q=+2$: about 0.030 eV upon addition of one electron to the V_O. This small shift contrasts with the larger shift of the deep level of the V_S, 0.460 eV from $Q=0$ to $Q=+1$ and 0.178 eV from $Q=+1$ to $Q=+2$. (Here the values of the energy shift are qualitatively meaning.) We can also explain this small energy shift from the strong hybridization between the yttrium atoms. Addition of electrons to a deep level usually causes an upward shift of the deep level due to Coulomb repulsion. However, when the electrons added occupies the ''bonding'' defect state, the deep level shifts downwards due to the stabilization of the orbital. The net level shift upon filling electrons to the deep level depends on the competition between the above energies. In the V_O, the hybridization of Y $4d$ states is so strong that the upward energy shift becomes small.

C. Atomic and electronic structures of interstitial anions

We discuss the atomic and electronic structures of the interstitial atoms in this subsection. Here, we focus mainly on the interstitial anions, because interstitial yttrium atom is expected to play a less important role than the interstitial anions because of its substantially larger DFE's (Fig. 2).

First we examine the geometries around the interstitial anions. Schematic views around interstitial anions are shown in Fig. 6. Positions of the interstitial anions remained at their initial positions during geometry optimization. The geometry information is also given in Tables III and IV. In our previous work, we compared the bond length and the sum of the corresponding Pauling's ionic radii[8] and confirmed that shorter bond length than the ionic radii sum mean that the bond is likely covalent.[7] We would like to stress that we can beforehand infer which kinds of bonds will appear around the interstitial anions to some extent with the help of the ionic radii in this case also. In all the charge states of the

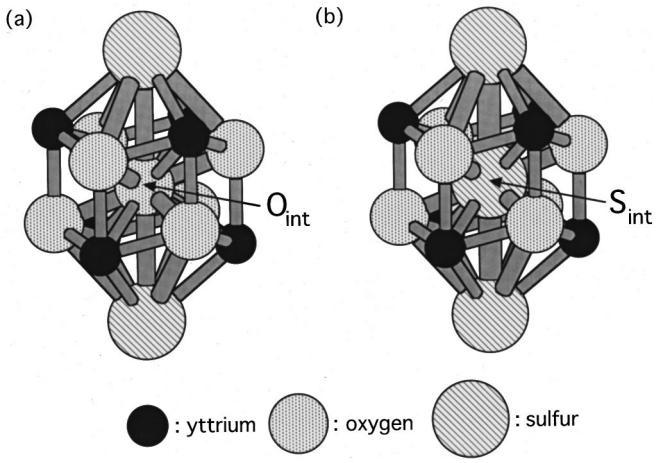

FIG. 6. Schematic views of atomic arrangements around (a) the interstitial oxygen atom and (b) the interstitial sulfur atom.

$O_{\rm int}$, the distances between the interstitial O and the neighboring Y atoms (ranging from 2.439 to 2.488 Å) are longer than the sum of Pauling's ionic radii of oxygen and yttrium ions (2.36 Å). This suggests that the bond between the interstitial oxygen and the neighboring yttrium atom is less covalent. On the contrary, in all the charge states of the $S_{\rm int}$, the distances between the interstitial sulfur and the neighboring Y atoms (ranging from 2.593 to 2.733 Å) are shorter than the sum of Pauling's ionic radii of sulfur and yttrium (2.80 Å). This suggests that the hybridization between the interstitial sulfur and the neighboring yttrium atoms is inevitably strong. This prospection is, in fact, supported by the relaxation energies from the ideal (initial) defect geometries to the final ones. When we compare the relaxation energy gain in neutral charge states, the energy gain in the $O_{\rm int}$ case (1.05 eV) is smaller than that in the $S_{\rm int}$ (1.44 eV). It means that the $O_{\rm int}$ feels not so cramped space to occupy the interstitial site in comparison to the other interstitial atom case.

Further, we have found interesting behaviors of the surrounding yttrium atoms when the charge states of the interstitial anions change; the more negatively charged the interstitial anion defect becomes, the shorter the distances between the interstitial anion and the neighboring yttrium cations, and at the same time the longer the distance between the interstitial anion and the neighboring oxygen anions become. At first sight, the direction of these displacements seems to be originate from the Coulombic interaction. Yet the magnitudes of the displacements of yttrium atoms are qualitatively different between the $S_{\rm int}$ and the $O_{\rm int}$; when the charge state of the interstitial anion changes from $Q=+2$ to -2, the displacement of the yttrium atom in $S_{\rm int}$ (0.186 Å) is much larger than the one in $O_{\rm int}$ (0.049 Å). From this observation, strong E-L coupling is also expected in the $S_{\rm int}$. This is in accord with the negative-U character in the DFE diagram of the $S_{\rm int}$ (Fig. 2). This difference can be expected from the difference in the distance between the interstitial atom and the surrounding yttrium atoms, as we explained before.

Next, we examine single-electron levels in the band gap induced by the interstitial anions. It is found that they are all doubly degenerate in the gap (Fig. 7); two electrons occupy the levels in the neutral charged state of both the $S_{\rm int}$ and $O_{\rm int}$. The $O_{\rm int}$ induce shallow acceptor levels, whereas $S_{\rm int}$ induce relatively deep levels. In addition, behaviors of the electron levels are very different when the charge state changes from $Q=+2$ to $Q=-2$; the levels of the $S_{\rm int}$ shift downwards, whereas the levels of the $O_{\rm int}$ shift upwards. This may be due to strong covalency between the interstitial sulfur and the neighboring yttrium atoms, as we have seen in the $V_{\rm O}$ case. The different characteristics between the $O_{\rm int}$ and the $S_{\rm int}$ are understood by observing wave functions of the electron levels (Fig. 8). We first notice the qualitative differences of the bonding between the $O_{\rm int}$ and the $S_{\rm int}$. In the $O_{\rm int}$ structure, the wave function are composed of delocalized p states of O and S atoms, which are in accord with the shallow acceptor nature of the $O_{\rm int}$ seen in Fig. 7. There seems no covalency between the $O_{\rm int}$ and the surrounding yttrium atoms and oxygen atoms at the defect level. On the other hand, the $S_{\rm int}$ induces relatively localized bonding states with the adjacent Y atoms and antibonding states with the adjacent O atoms. As a result, the bonding character between the $S_{\rm int}$-p and the Y-d levels makes the defect level relatively deep in the gap. The strong hybridization around the interstitial sulfur atom can lead to the negative-U character of the $S_{\rm int}$.

IV. DISCUSSION

In this section, we try to give microscopic explanations of experimental results available, based on the calculated results. We discuss (1) the p-type photoconductivity under UV-light, (2) long-lasting phosphorescence and energy storage effects in Eu-doped oxysulfides, and (3) broad-band blue fluorescence (around 355 and 440 nm) under electron beam irradiation, as are explained in the Introduction.

Coexistence of shallow acceptor levels and deep levels seems to be a key to explain the above experiments. Regarding the shallow acceptor levels that can explain p-type pho-

TABLE III. The distances between the interstitial sulfur ($S_{\rm int}$) site and the neighboring atoms in the total-energy minimized interstitial sulfur. Superscripts stand for charge states of the $S_{\rm int}$. The distances in the initial (unrelaxed) configuration and sum of Pauling's ionic radii are also shown in the columns ''$S_{\rm int}^{(\rm init)}$'' and ''ionic radii sum,'' respectively. As for ionic radii, we adopted 0.96, 1.40, and 1.84 Å for yttrium, oxygen, and sulfur atoms, respectively. Units in Å .

Parameters	$S_{\rm int}^{(+2)}$	$S_{\rm int}^{(+1)}$	$S_{\rm int}^{(0)}$	$S_{\rm int}^{(-1)}$	$S_{\rm int}^{(-2)}$	$S_{\rm int}^{(\rm init)}$	Ionic radii sum
$S_{\rm int}$-Y	2.733	2.678	2.633	2.591	2.547	2.593	2.80
$S_{\rm int}$-O	2.260	2.357	2.418	2.472	2.531	2.324	3.24
$S_{\rm int}$-S	3.326	3.313	3.256	3.321	3.343	3.263	3.68

TABLE IV. The distances between the interstitial oxygen (O_{int}) site and the neighboring atoms in the interstitial oxygen. Superscripts stand for charge states of O_{int}. The distances in the initial configuration and sum of Pauling's ionic radii are also shown in the columns ''$O_{int}^{(init)}$'' and ''ionic radii sum,'' respectively. As for ionic radii, we adopted 0.96, 1.40, and 1.84 Å for yttrium, oxygen, and sulfur atoms, respectively. Units in Å.

Parameters	$O_{int}^{(+2)}$	$O_{int}^{(+1)}$	$O_{int}^{(0)}$	$O_{int}^{(-1)}$	$O_{int}^{(-2)}$	$O_{int}^{(init)}$	Ionic radii sum
O_{int}-Y	2.488	2.484	2.477	2.463	2.439	2.593	2.36
O_{int}-O	2.430	2.437	2.441	2.454	2.466	2.324	2.80
O_{int}-S	3.271	3.272	3.256	3.292	3.304	3.263	3.24

toconductivity under UV-light, we argue that the O_{int} is the most probable candidate, because it induces shallow levels and its DFE is the smallest in the all intrinsic defects in almost all range of μ_e. This shallow acceptor levels induced by the O_{int} may also be responsible for the persistent phosphorescence and the energy storage effects.

Deep levels are certainly responsible for the broad-band blue fluorescence. Since two peaks in the spectra (3.5 and 2.8 eV) are observed, we expect that more than one deep levels are related to the spectra. From the broadness of the spectra, the transition between the deep levels and the shallow acceptor levels may also be expected. Unfortunately, there have been no experimental results to identify the deep levels directly. Based on our calculated DFE's, we argue that the V_O, the V_S, and the S_{int} are the plausible candidates being responsible for the deep levels. We also mention that the V_S can be detected by magnetic resonance experiments, because there is a range of electron chemical potential where the V_S has an unpaired electron (Fig. 2).[34]

We also mention broad-band yellow luminescence observed in Ca-doped $(Y_{1-x},Gd_x)_2O_2S$ by Kano.[35] He speculated that doped Ca^{+2} cations may substitute Y^{+3} and can be shallow acceptors, which also induce anion vacancies for charge compensation as a whole system. In Kano's original paper,[35] he supposed that the Ca-acceptor levels capture holes and produce the yellow luminescence due to recombination with ''excited electrons,'' which have a localized character. The charge compensation mechanism is expected from our DFE diagrams, because Ca-doping renders the electron chemical potential come closer to the valence-band top where the DFE's of the anion vacancies (and the interstitial sulfur) become smaller. Once the anion vacancy (or possibly the interstitial sulfur) is formed, his picture of localized ''excited electrons'' are the deep levels of the V_O and the V_S (or the S_{int}); the wave functions of the anion vacancies and the interstitial sulfur are relatively localized, which come mainly from the localized yttrium $4d$ orbitals. However, in order to clarify his microscopic model, further experimental works and theoretical works should be necessary.

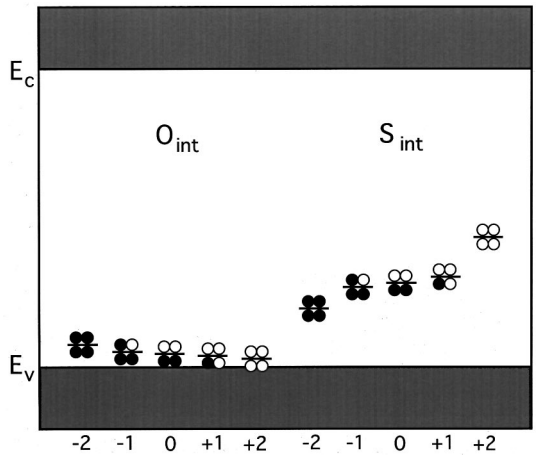

FIG. 7. Single-electron levels in the energy gap induced by the interstitial oxygen and sulfur atoms. The signed numbers stand for charge states of the defects. Filled circles indicate electrons, and open circles indicate holes.

V. CONCLUSION

The electronic structure of point defects (vacancies and interstitial atoms) in Y_2O_2S is investigated, based on the pseudopotential-density-functional method in a supercell geometry. We have found that the anion-related defects are abundant in real materials. Interstitial oxygen induces relatively shallow acceptor levels, which are likely to be related to the *p*-type photoconductivity, and presumably persistent phosphorescence and energy storage phenomena in Eu-doped oxysulfides. An oxygen vacancy, a sulfur vacancy, and an interstitial sulfur induce the deep levels in the band gap, which are responsible for the broad-band blue luminescence observed in nominally undoped yttrium oxysulfide. Further, negative-*U* behaviors are found in the oxygen vacancy and the interstitial sulfur atom. When the charge state of the oxygen vacancy changes, energy shift of the deep level is found to be small. These behaviors can be explained from the viewpoint of ''covalency'' of the bonds, which newly appear among the surrounding atoms or among the

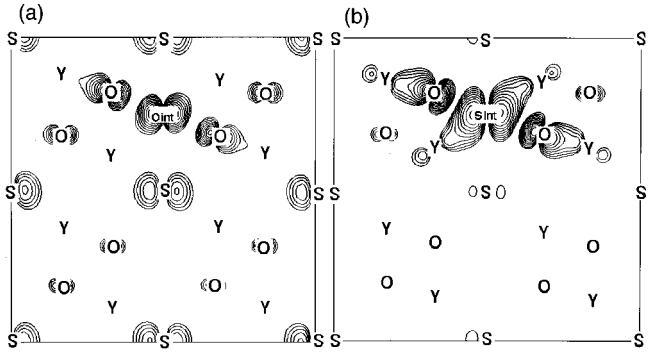

FIG. 8. Contour maps of wave functions of the defect levels for the interstitial oxygen and sulfur atoms at Γ point; (a) interstitial oxygen and (b) interstitial sulfur. The subsequent contours represent the values different to each other by a factor of 1.5.

interstitial and the neighboring atoms. Especially, the idea of ''Pauling's ionic radius'' can help to predict the covalency between interstitial anions and the neighboring yttrium atoms.

In our previous work,[7] we expected the different physical and/or chemical properties between the oxygen vacancy and the sulfur vacancy. It is now clarified that the differences are due to the competition between covalency and ionicity around the defects. We could expect the similar defect-related properties in other oxysulfides, because they belong to the same space group and are known to be chemically similar systems.

ACKNOWLEDGMENTS

We wish to acknowledge K. Kobayashi and M. Arai for helpful discussions, particularly in the determination of our yttrium pseudopotential. M.M. wishes to thank H. Yamamoto, T. Fujiwara, S. Nakamura, and Y. Oguri for stimulating discussions and continual encouragements. The series of the calculations were done by Fujitsu VX-1S.

*Electronic address: mmikami@rc.m-kagaku.co.jp

[1] S. Kim, I. P. Herman, J. A. Tuchman, K. Doverspike, L. B. Rowland, and D. K. Gaskill, Appl. Phys. Lett. **67**, 380 (1995); E. R. Glaser, T. A. Kennedy, K. Doverspike, L. B. Rowland, D. K. Gaskill, J. A. Freitas, Jr., M. Asif Khan, D. T. Olson, J. N. Kuznia, and D. K. Wickenden, Phys. Rev. B **51**, 13 326 (1995); T. Suski, P. Perlin, H. Teisseyre, M. Leszczyński, I. Grzegory, J. Jun, M. Boćkowski, S. Porowski, and T. D. Moustakas, Appl. Phys. Lett. **67**, 2188 (1995); D. M. Hofmann, D. Kovalev, G. Stende, B. K. Meyer, A. Hoffman, L. Eckey, R. Heitz, T. Detchprom, H. Ameno, and J. Akasaki, Phys. Rev. B **52**, 16 702 (1995).

[2] C. G. Van de Walle, Phys. Rev. B **56**, R10 020 (1997); J. Neugebauer and C. G. Van de Walle, Appl. Phys. Lett. **69**, 503 (1996).

[3] G. Czack, H. Hein, I. Hinz, H. Bergmann, and P. Kuhn, in *Gmelin Handbook of Inorganic Chemistry*, edited by G. Czack, H. Hein, G. Kirschstein, P. Merlet, and U. Vetter (Springer-Verlag, Berlin, 1983), Chap. 7, p. 560.

[4] For examples, G. Blasse and B. C. Grabmaier, *Luminescent Materials* (Springer-Verlag, Berlin, 1994); B. Smets, in *Advances in Nonradiative Processes in Solids*, edited by B. Di Bartolo (Plenum Press, New York, 1991); S. Shionoya and W. M. Yen, *Phosphor Handbook* (CRC, Boca Raton, FL, 1998).

[5] M. R. Royce and A. L. Smith (unpublished); M. R. Royce, U.S. Patent No. 3.4.18.246 (1968).

[6] S. S. Trond, J. S. Martin, J. P. Stanavage, and A. L. Smith, J. Electrochem. Soc. **116**, 1047 (1969).

[7] M. Mikami and A. Oshiyama, Phys. Rev. B **57**, 8939 (1998).

[8] For example, L. Pauling, *The Nature of the Chemical Bond*, 3rd ed. (Cornell University Press, Ithaca, NY, 1960).

[9] W. I. Dobrov and R. A. Buchanan, Appl. Phys. Lett. **21**, 201 (1972).

[10] C. W. Struck and W. H. Fonger, in *Optical Properties in Excited States in Solids*, Vol. 301 of *NATO Advanced Studies Institute, Series B: Physics*, edited by B. D. Bartolo (Plenum Press, New York, 1992), p. 479, and references therein.

[11] H. Forest, A. Cocco, and H. Hersh, J. Lumin. **3**, 25 (1970).

[12] W. H. Fonger and C. W. Struck, J. Electrochem. Soc. **118**, 273 (1971).

[13] H. Yamamoto and H. Matsukiyo, Proc. SPIE **2362**, 612 (1995).

[14] C. H. Park and D. J. Chadi, Phys. Rev. B **55**, 12 995 (1997).

[15] T. Mattila and R. M. Nieminen, Phys. Rev. B **55**, 9571 (1997).

[16] D. C. Allan and M. P. Teter, J. Am. Ceram. Soc. **73**, 3247 (1990).

[17] A. Oshiyama, Jpn. J. Appl. Phys., Part 2 **37**, L232 (1998).

[18] M. Boero, A. Pasquarello, J. Sarnthein, and R. Car, Phys. Rev. Lett. **78**, 887 (1997).

[19] P. Hohenberg and W. Kohn, Phys. Rev. **136**, B864 (1964).

[20] W. Kohn and L. J. Sham, Phys. Rev. **140**, A1133 (1965).

[21] M. C. Payne, M. P. Teter, D. C. Allan, T. A. Arias, and J. D. Joannopoulos, Rev. Mod. Phys. **64**, 1045 (1992).

[22] A. Oshiyama and M. Saito, J. Phys. Soc. Jpn. **56**, 2104 (1987); O. Sugino and A. Oshiyama, Phys. Rev. Lett. **68**, 1858 (1992); M. Saito, O. Sugino, and A. Oshiyama, Phys. Rev. B **46**, 2606 (1992).

[23] N. Troullier and J. L. Martins, Phys. Rev. B **43**, 1993 (1991).

[24] L. Kleinman and D. M. Bylander, Phys. Rev. Lett. **48**, 1425 (1982).

[25] D. M. Ceperley and B. J. Alder, Phys. Rev. Lett. **45**, 556 (1980).

[26] J. P. Perdew and A. Zunger, Phys. Rev. B **23**, 5048 (1981).

[27] Convergence of the results with respect to the supercell size is not fully examined in the present work. The next larger supercell containing 80 lattice sites is impossible to treat in our current computation resources.

[28] We have found that adequate cutoff energies for sulfur, oxygen and yttrium pseudopotentials are 25, 59, and 40 Ry, respectively, by computing the total energies as a function of the cutoff energy for several reference materials. As for our yttrium and sulfur pseudopotentials, we have checked their reliabilities, for example, through yttrium sulfide (YS) calculation: the calculated lattice constants are 1.4% smaller than the experimental value with 40-Ry energy cutoff. As for oxygen, we performed electronic structure calculations for alpha quartz, and found that the lattice constants are 0.3% smaller than the experimental values with 59-Ry cutoff. Further details can be found in Refs. 7 and 17.

[29] D. J. Chadi and M. L. Cohen, Phys. Rev. B **8**, 5747 (1973).

[30] D. C. Patton, D. V. Porezag, and M. R. Pederson, Phys. Rev. B **55**, 7454 (1997).

[31] If we set μ_O by the formation of oxides with yttrium, i.e., $2\mu_Y + 3\mu_O = \mu_{Y_2O_3}$, the chemical potentials of oxygen and yttrium change by about -2.4 and $+1.2$ eV, respectively. When we adopt these values, we find that the DFE's of V_Y and Y_{int} are higher than other DFE's. The conclusion in this paper described in the text is thus unchanged.

[32] As for a general reference of Slater's transition state theory, see, J. C. Slater, *The Self Consistent Field for Molecules and Solids* (McGraw-Hill, New York, 1974); *The Calculation of Molecular Orbitals* (Wiley, New York, 1979). The Slater transition-state can be applied to an estimate of the total energy change caused by addition of a single electron at fixed configuration in solids. For example, see G. A. Baraff, E. O. Kane, and M. Schlüter, Phys. Rev. B **21**, 5662 (1980); G. A. Baraff, M. Schlüter, and G. Allen, Phys. Rev. Lett. **50**, 739 (1983). When two systems with the same atomic geometry have charge states Q and $Q-1$, respectively, the total energy difference between them is given as the highest occupied level ϵ of a system having $Q-0.5$ charge

with the same atomic geometry: $E(Q)-E(Q-1)=\epsilon(Q-0.5)+o(\partial^3 E/\partial Q^3)$. In order to obtain the relative total energy of a charge state Q having a different atomic geometry from the state $Q-1$, we first calculate ϵ of the state $Q-0.5$, and $E_{\rm tot}(Q)'$ of the state Q, keeping atomic geometries the same as that of the state $Q-1$. The total energy difference $E_{\rm tot}(Q)'-E_{\rm tot}(Q-1)$ is then replaced by ϵ. On the other hand, the total energy lowering dE (positive definition), after optimizing the atomic geometry of the state Q, can be obtained by $E_{\rm tot}(Q)'-E_{\rm tot}(Q)$. Here, $E_{\rm tot}(Q)$ is a total energy of the charge state Q after the geometry optimization. After all, the relative total energy of the geometry-optimized Q state compared to the state $Q-1$, $E_{\rm tot}(Q)-E_{\rm tot}(Q-1)$, is evaluated as $\epsilon-dE$. Since $E_{\rm tot}(0)$ is well defined, we can inductively determine the total energy of the charge state Q, $E_{\rm tot}(Q)$.

[33] There are no experimental data to be compared with the DFE of $V_{\rm O}$ (5.93 eV), but it is smaller than the calculated DFE in α quartz, 6.6 eV (Ref. 17) or 7.85 eV (Ref. 16).

[34] Tamatani *et al.* reported F centers in Y_2O_2S using magnetic resonance method; M. Tamatani, N. Tsuda, K. Nomoto, T. Nishimura, and K. Yokota, J. Lumin. **12/13**, 935 (1976).

[35] T. Kano, J. Lumin. **29**, 177 (1984).